KSME International Journal, Vol. 15 No. 8, pp. 1165~1173, 2001

Modeling and Simulation for PIG Flow Control in Natural Gas Pipeline

Tan Tien Nguyen*, Sang Bong Kim
Department of Mechanical Eng., Pukyong National University, Pusan 608-739, Korea
Hui Ryong Yoo, Yong Woo Rho
Korea Gas Corporation (KOGAS) 638, Il-dong, Kyungyi-do, 425-160, Korea

This paper deals with dynamic analysis of Pipeline Inspection Gauge (PIG) flow control in natural gas pipelines. The dynamic behaviour of PIG depends on the pressure differential generated by injected gas flow behind the tail of the PIG and expelled gas flow in front of its nose. To analyze dynamic behaviour characteristics (e.g. gas flow, the PIG position and velocity) mathematical models are derived. Two types of nonlinear hyperbolic partial differential equations are developed for unsteady flow analysis of the PIG driving and expelled gas. Also, a non-homogeneous differential equation for dynamic analysis of the PIG is given. The nonlinear equations are solved by method of characteristics (MOC) with a regular rectangular grid under appropriate initial and boundary conditions. Runge-Kutta method is used for solving the steady flow equations to get the initial flow values and for solving the dynamic equation of the PIG. The upstream and downstream regions are divided into a number of elements of equal length. The sampling time and distance are chosen under Courant-Friedrich-Lewy (CFL) restriction. Simulation is performed with a pipeline segment in the Korea gas corporation (KOGAS) low pressure system, Ueijungboo-Sangye line. The simulation results show that the derived mathematical models and the proposed computational scheme are effective for estimating the position and velocity of the PIG with a given operational condition of pipeline.

Key Words: Pipeline Inspection Gauge (PIG), Method Of Characteristics (MOC)

Nomenclature

A : Pipe cross section area [m²]
c : Wave speed [m/s]
C : Linear damping coefficient of PIG [Ns/m]
C_c : Convection heat transfer coefficient [W/m² K]
C_v : Specific heat at constant volume [J/kgK]
d : Internal diameter of pipe [m]
e : Internal energy per unit mass [J/kg]
f : Darcy friction coefficient
F_b : Braking force [N]
F_f : Friction force per unit pipe length [N/m]
F_{fp} : Friction force between PIG and pipe wall including [N]
F_{fpsta} : Static friction force
F_{fpdyn} : Dynamic friction force
F_p : PIG driving force [N]
g : Gravity acceleration [m/s²]
h_f : Pipe head loss [m]
k : Pipe wall roughness [m]
K : Wear factor per distance travel [N/m]
l : Length of pipeline [m]
L_{PIG} : Length of PIG [m]
m : Hydraulic mean radius of pipe [m]
M : Weight of PIG [kg]

* Corresponding Author,
E-mail : tiennt@yahoo.com
TEL : +82-51-620-1606; **FAX** : +82-51-621-1411
Department of Mechanical Eng., Pukyong National University, Pusan 608-739, Korea.(Manuscript **Received** August 7, 2000; **Revised** May 9, 2001)

p : Flow pressure [N/m^2]
q : Compound rate of heat inflow per unit area of pipe wall [W'/m^2]
R : Gas constant [J/kgK]
S : Perimeter of pipe [m]
T : Flow temperature [K]
T_{ext} : Seabed temperature [K]
u : Flow velocity [m/s]
x : Distance from pipe inlet [m]
x_{PIG} : Position of PIG [m]
v_{PIG} : Velocity of PIG [m/s]

Greeks

γ : The ratio of specific heat
ν : Kinetic viscosity of flow [m^2/s]
ρ : Fluid density [kg/m^3]

Subscripts

L, R, M, N, S, O, P: The grid points, and
0, l : The points at inlet and outlet of pipeline

1. Introduction

Pipelines are the most common way and the safest method to transport oil and gas products. During operation, the walls of pipelines suffer a deterioration process and pipeline conditions get worse. Therefore, the pipeline's hydraulic efficiency decreases and it leads to more high operation expensive due to the high pumping costs. The reduction of the efficiency results from two factors: the increase of pipe wall's roughness and the reduction of the internal diameter. To prevent above factors, pipeline must be pigged regularly. The tool used for pigging is called Pipeline Inspection Gauge (PIG). The PIG is a device which is inserted into a pipeline and travels throughout the pipeline to be inspected. It plays a major role in pipeline operation such as maintaining continuous operation and maximum efficiency by removing any debris and deposit restricting the flow. Furthermore, it plays a role in monitoring the physical conditions of the pipeline. The PIG is the most effective when it runs at a near constant speed but will not be effective when it runs at too high speed. The typical speeds for pigging are about 1-5 m/s for on-stream liquids and 2-7 m/s for on-stream gas (Cordell and Vanzout, 1999). So, prediction of the velocity of the PIG is very important before we operate it.

The PIG is driven by injected gas flow behind its tail and expelled gas flow in front of its nose. That is, the dynamics behaviour of the PIG depends on the different pressure across its body. To estimate the velocity of the PIG, the transient mathematical models are formulated as the following two models:

- Unsteady flow analysis of the PIG driving gas and of the expelled gas.
- Dynamics analysis of the PIG.

To understand the dynamic behaviour of the PIG, the governing nonlinear hyperbolic partial differential equations of flows must be solved together with the PIG dynamic equation. Results of research on the motion of the PIG in pipeline are scarcely found in the literatures. Some works relating to this subject have been reported. Azevedo et al. (1995), simplified the solution with assumption of incompressible and steady state of flow. J. M. M. Out (1993), used Lax-Wendroff scheme for the integration of gas equations with adaptation of finite difference grid. The grid has to be continuously updated with the PIG position and the flow values at the new grid points are estimated by interpolation. P. C. R. Lima (1999), solved this problem by using one-dimensional semi-implicit finite difference scheme. The nonlinear algebraic equations at each time step are solved by adopting Newton's method. In this paper, we use method of characteristics (MOC) with regular rectangular grid to solve the problem. Usually, MOC is used to solve the nonlinear hyperbolic partial differential equations (J. A. Fox, 1977; E. B. Wylie et al., 1993; J. A. C. Kentfield, 1993; B. K. Hodge and K. Koenig, 1995; W. G. Sim and J. H. Park, 1997). This method is employed to transform partial differential equations (PDE) to ordinary differential equations (ODE). The ODEs are then integrated along the corresponding characteristic lines to generate a set of explicit finite differential representations to be evaluated with suitable

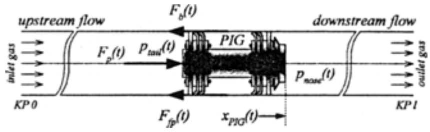

Fig. 1 PIG flow in the natural gas pipeline

conditions. This approach is quite efficient for modelling the rapid flow transient. The reliability and accuracy of this method can be found in references. The simulation results in this paper also show that the solution for PIG dynamics problem by using MOC with proposed computational scheme is converged with appropriate small sampling time and distance.

The gas upstream and downstream of the PIG are divided into a number of elements of equal length. The sampling distance and time are chosen under the Courant-Friedrich-Lewy (CFL) restriction. For each gas element, the flow fundamental equations are solved to give the change in the flow dynamics at the end of a time step. The gas pressures at the front and tail of the PIG are then calculated. From these pressures, the PIG driving force is derived and its dynamic equation is solved to get its position and velocity. With the calculated values for the PIG dynamics, we derive the boundary conditions at its tail and nose, and use these values when we solve the flow dynamics. The gas flow and the PIG dynamics calculations are repeated until the PIG arrives at the end of pipeline.

2. Modeling

The scheme of PIG flow in pipeline is given in Fig. 1.

2.1 Gas flow model

2.1.1 Governing dynamic equations

We assume as the following:

(1) the natural gas is ideal and flow is one phase,

(2) pipeline internal diameter is constant, and the pipe wall thickness is large enough to ignore the radial deformation,

(3) the pipe center line is in a horizontal or near horizontal line to ignore the effect of gravity.

(4) the friction factor is a function of wall roughness and Reynolds number. Steady state values are used in transient calculations,

(5) the flow of gas is quasi-steady heat flow.

The unsteady flow dynamics can be modelled based on four fundamental fluid dynamic equations: continuity equation, momentum equation, state equation and energy equation respectively as follows:

$$\frac{\partial \rho}{\partial t}+u\frac{\partial \rho}{\partial x}+\rho\frac{\partial u}{\partial x}=0 \tag{1}$$

$$\frac{\partial p}{\partial x}+\rho u\frac{\partial u}{\partial x}+\rho\frac{\partial u}{\partial t}+\frac{F_f}{A}=0 \tag{2}$$

$$\frac{p}{\rho}=RT=(\gamma-1)C_vT \tag{3}$$

$$\frac{\partial}{\partial t}\left[\rho\left(e+\frac{u^2}{2}\right)\right]+\frac{\partial}{\partial x}\left[\rho u\left(e+\frac{u^2}{2}\right)\right]+\frac{\partial}{\partial x}(pu)-\frac{qS}{A}=0 \tag{4}$$

The fluid variables p, ρ, u must be solved at each location x and time t. The value of F_f is calculated as shown in Appendix. The mathematical description of the heat rate term, q, in Eq. (4) is dependent on the problem assumptions. Because there is no heat producing in flow, q could be evaluated as a quasi-steady heat transfer from the surrounding environment to the gas:

$$q=C_c(T_{ext}-T) \tag{5}$$

With assumption of ideal gas, internal energy per unit mass can be given by $e=C_vT$. Using Eq. (3), we can rewrite Eq. (4) in the following form:

$$\frac{\partial p}{\partial t}+u\frac{\partial p}{\partial x}+\gamma p\frac{\partial u}{\partial x}=\frac{\gamma-1}{A}(F_fu+qS) \tag{6}$$

Eqs. (1), (2) and (6) can be rewritten in the following form:

$$\frac{\partial \boldsymbol{u}}{\partial t}+A\frac{\partial \boldsymbol{u}}{\partial x}=\boldsymbol{B} \tag{7}$$

where,

$$\boldsymbol{u}=[\rho\ \ u\ \ p]^T,$$

$$A=\begin{bmatrix} u & \rho & 0 \\ 0 & u & \dfrac{1}{\rho} \\ 0 & \gamma p & u \end{bmatrix},\ \boldsymbol{B}=\begin{bmatrix} 0 \\ -\dfrac{F_f}{\rho A} \\ \dfrac{\gamma-1}{A}(F_f u+qS) \end{bmatrix}.$$

The nonlinear hyperbolic partial differential system of equations [Eq. (7)] is transformed into ODEs which can be integrated by finite differences. Matrix A has 3 real eigenvalues λ:

$$\lambda=[u,\ u+c,\ u-c],\ c=\sqrt{\frac{\gamma p}{\rho}}$$

and we can choose the corresponding left eigenvectors v:

$$v=\begin{bmatrix} \begin{bmatrix} \dfrac{u}{\rho} \\ 0 \\ -\dfrac{u}{\gamma p} \end{bmatrix} & \begin{bmatrix} 0 \\ 1 \\ \dfrac{c}{\gamma p} \end{bmatrix} & \begin{bmatrix} 0 \\ 1 \\ -\dfrac{c}{\gamma p} \end{bmatrix} \end{bmatrix}$$

For each pair of λ and v, Eq. (7) can be rewritten in the form:

$$v^T\frac{d\boldsymbol{u}}{dt}=v^T\boldsymbol{B} \tag{8}$$

along the characteristic line:

$$\frac{dx}{dt}=\lambda(x,\ t,\ u) \tag{9}$$

From Eqs. (8) and (9), Eq. (7) now becomes

$$\frac{du}{dt}+\frac{c}{\gamma p}\frac{dp}{dt}=E_1 \text{ along } \frac{dx}{dt}=u+c \tag{10}$$

$$\frac{du}{dt}-\frac{c}{\gamma p}\frac{dp}{dt}=E_2 \text{ along } \frac{dx}{dt}=u-c \tag{11}$$

$$\frac{dp}{dt}-c^2\frac{d\rho}{dt}=E_3 \text{ along } \frac{dx}{dt}=u \tag{12}$$

where,

$$E_1=\frac{\gamma-1}{c}\frac{q}{\rho m}+\frac{F_f}{\rho A}\left[\frac{u(\gamma-1)}{c}-1\right] \tag{13}$$

$$E_2=-\frac{\gamma-1}{c}\frac{q}{\rho m}-\frac{F_f}{\rho A}\left[\frac{u(\gamma-1)}{c}+1\right] \tag{14}$$

$$E_3=(\gamma-1)\left(\frac{q}{m}+\frac{F_f u}{A}\right) \tag{15}$$

with m=A/S. Here we use finite differences with the regular rectangular grid. The sampling distance, Δx, and the sampling time, Δt, are chosen under the CFL stability constrain (Tannehill et al., 1997):

$$\Delta t<\left|\frac{\Delta x}{u\pm c}\right| \tag{16}$$

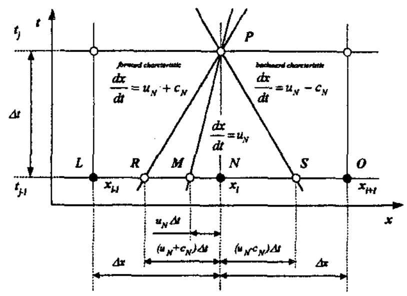

Fig. 2 Backward and forward characteristics using in MOC

Figure 2 shows the relationship between fluid variables p, ρ, u at the time step t_j and at preceeding time step t_{j-1}. Using Eqs. (10)~(12) under description of variables shown in Fig. 2, we can derive the variables p, ρ, u at grid point P from previous calculated grid points L, N, and O. Firstly, we get flow parameters at grid points R, M, S from linear interpolation formula. Then, we integrate Eqs. (10)~(12) along the corresponding characteristic lines dx/dt to get the desired variables.

$$X_R=X_N-(X_N-X_L)\frac{(u_N+c_N)\Delta t}{\Delta t} \tag{17}$$

$$X_M=X_N-(X_N-X_L)\frac{u_N\Delta t}{\Delta x} \tag{18}$$

$$X_S=X_N-(X_N-X_O)\frac{(u_N-c_N)\Delta t}{\Delta x} \tag{19}$$

$$p_P=\frac{\gamma}{\dfrac{c_R}{p_R}+\dfrac{c_S}{p_S}}\times \left[(u_R-u_S)+\frac{c_R+c_S}{\gamma}+(E_{1R}-E_{2S})\Delta t\right] \tag{20}$$

$$u_P=u_R+\frac{c_R}{\gamma p_R}(p_R-p_P)+E_{1R}\Delta t \tag{21}$$

$$\rho_P=\rho_M+\frac{1}{c_M^2}[p_P-p_M-E_{3M}\Delta t] \tag{22}$$

In Eqs. (17)~(19), X will be replaced by the desired calculating values p, ρ or u. And E_{1R}, E_{2S}, E_{3M} in Eqs. (20)~(22) can be calculated from Eqs. (13)~(15) at the corresponding grid points R, S, and M.

2.1.2 Initial conditions

In the absence of field data concerning the initial field variable distributions, it is assumed that steady state variable distributions are used for the initial conditions. These values can be obtained by using the analytical Eqs. (1), (2) and (6):

$$u\rho=\text{constant} \tag{23}$$

$$\frac{du}{dx}=-\frac{1}{\rho(u^2-c^2)}\left[\gamma\frac{F_f u}{A}+(\gamma-1)\frac{q}{m}\right] \tag{24}$$

$$\frac{dp}{dx}=-\frac{F_f}{A}+\frac{u}{u^2-c^2}\left[\gamma\frac{F_f u}{A}+(\gamma-1)\frac{q}{m}\right] \tag{25}$$

The Runge-Kuta method is used for solving the above equations to get the initial fluid variables $\rho(0, x)$, $u(0, x)$ and $p(0, x)$ at the given grid points for both upstream and downstream flows.

2.1.3 Boundary conditions

The boundary conditions at pipeline inlet and outlet can be given in two ways: under a condition of flow rate $Q(t)$ or pressure $p(t)$ together with the temperature of fluid $T(t)$. The boundary conditions at the tail of the PIG for upstream flow and at its nose for downstream flow depend on dynamics behaviour of the PIG, such as its position, $x_{PIG}(t)$, and its velocity, $v_{PIG}(t)$. At a boundary there is only one available characteristic such as a backward characteristic at an upstream boundary or a forward characteristic at an downstream boundary. The unsteadiness is initiated from the boundaries. Therefore, to choose appropriately boundary conditions is very important. We will consider the boundaries at inlet and out let of pipeline, also at the tail and nose of the PIG.

2.1.3.1 Given flow rate at pipe inlet and outlet

Flow velocity is calculated from flow rate:

$$u(t)=Q(t)/A \tag{26}$$

At the pipeline inlet, the backward characteristic is used to calculate the pressure p_P at grid point P from available data at grid points N and O as shown in Fig. 2. From Eq. (11), we can obtain:

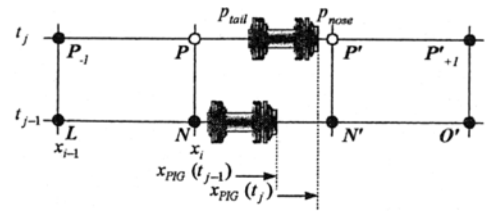

Fig. 3 Scheme for calculation of boundary values at the tail and the nose of the PIG (PIG stays in same grid space)

$$p_P=p_S+\frac{\gamma p_S}{c_S}[(u_P-u_S)-E_{2S}\Delta t] \tag{27}$$

At pipeline outlet, the forward characteristic is used for calculation of the pressure p_P at grid point P from available data at points L and N as shown in Fig. 2. From Eq. (10), we can get:

$$p_P=p_R+\frac{\gamma p_R}{c_R}[-(u_P-u_R)+E_{1R}\Delta t] \tag{28}$$

2.1.3.2 Given pressure at pipe inlet and outlet

In the case of given pressure boundary condition, flow velocity u_P is calculated at the pipeline inlet and outlet, respectively:

$$u_P=u_S+\frac{c_S}{\gamma p_S}(p_P-p_S)+E_{2S}\Delta t \tag{29}$$

$$u_P=u_R-\frac{c_R}{\gamma p_R}(p_P-p_R)+E_{1R}\Delta t \tag{30}$$

2.1.3.3 Boundary conditions at PIG tail and nose

With the assumption that the upstream and downstream flows are completely decoupled by the PIG, flow velocities at its tail and its nose equal to its velocity. If the PIG does not move to next grid space, we can interpolate to get flow velocity at point P as follows:

$$u_P=u_{P-1}+\frac{x_{P-1}-x_P}{x_{P-1}-x_{tail}}(v_{PIG}-u_{P-1}) \tag{31}$$

Using this value and Eq. (28) to derive pressure at P, then we extrapolate to get the pressure at the tail of the PIG as follows:

$$p_{tail}=p_{P-1}+\frac{x_{P-1}-x_{tail}}{x_{P-1}-x_P}(p_P-p_{P-1}) \tag{32}$$

The PIG can move to the next grid space as

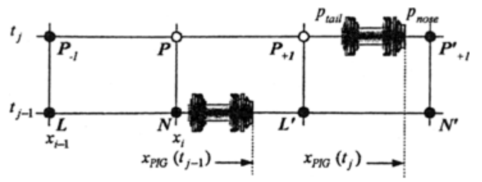

Fig. 4 Scheme for calculation of boundary values at the tail of the PIG(PIG moves to the next grid space)

shown in Fig. 4. In this case, after calculation of pressure at the tail of the PIG, flow parameters at point P_{+1} must be derived for the next step calculation.

The way of calculation flow parameters at the nose of the PIG is the same one which has done at its tail. Flow velocity at P' and the pressure at the nose of the PIG are given by the following:

$$u_{P'}=v_{PIG}+\frac{x_{PIG}-x_{P'}}{x_{PIG}-x_{P'+1}}(u_{P'+1}-v_{PIG}) \quad (33)$$

$$p_{nose}=p_{P'}+\frac{x_{P'}-x_{PIG}}{x_{P'}-x_{P'+1}}(p_{P'+1}-p_{P'}) \quad (34)$$

If the PIG moves to next grid space, flow parameters at grid point P' are calculated using Eqs. (17)-(22). Then Eq. (34) is used to derive the pressure at the nose of the PIG.

2.2 PIG dynamics model

Forces acting on the PIG are shown in Fig. 1. The dynamic equation of the PIG can be written from the Newton's Second Law as follows:

$$M\frac{d^2x}{dt^2}+C\frac{dx}{dt}+Kx=F_p(t)+F_{fp}(t)+F_b(t) \quad (35)$$

In the above equation, the driving force $F_p(t)$ is derived from the differential pressure at the tail and the nose of the PIG which are calculated from upstream and downstream flow dynamics in each computational step. The friction force $F_{fp}(t)$ between the PIG and pipeline wall is assumed to be constant including static and dynamic friction forces. The braking force $F_b(t)$ is applied to the PIG when it is reaching near to the end of pipeline to attain its stopping at its trap barrel. The wear factor, K, includes static wear factor and dynamic wear factor. The values of K, C and F_{fp} are measured from experiment. The position

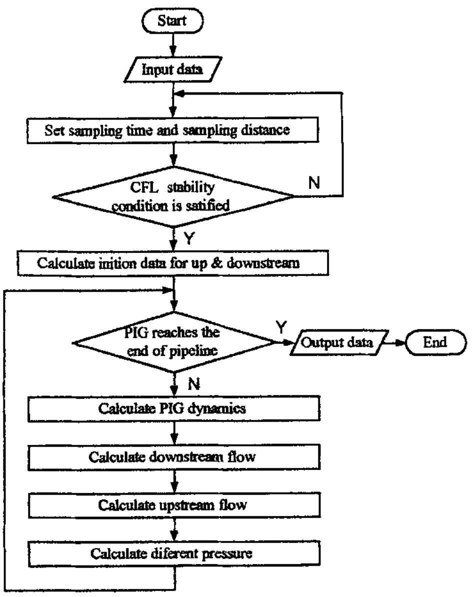

Fig. 5 Computational scheme

and velocity of the PIG can be calculated from Eq. (35) by using Range-Kuta method.

3. Computational Scheme

The steps of computing the PIG dynamics are simplified by the computational scheme shown in Fig. 5.

Fist of all, the sampling distance and time are chosen and the CFL condition (16) must be checked to make sure whether the computing is stable or not. Then the initial values at grid points along pipeline are calculated for both upstream and downstream flows. If the PIG does not reach the end of pipeline yet, the dynamics of the PIG is calculated. From the new position and velocity of the PIG, the dynamics of upstream and downstream of flows are derived to get the gas pressure at the front and the tail of the PIG. Then the different pressure now is derived to calculate the PIG movement in next time step. The flow dynamic characteristics and the PIG calculations are repeated for further time steps until the PIG reaches the end of pipeline.

Table 1 Numerical values for simulation

Parameters	Values	Units	Parameters	Values	Units
l	14,800	m	ν	1.45e-5	m^2/s
d	0.7366	m	R	518.30	J/kgK
k	0.0450	mm	γ	1.40	
C_c	2	W/m^2K	M	2320	kg
T_{ext}	15	℃	C	0.74	Ns/m
p_0	8	bar	K	0.00	N/m
Q_0	1.16	m^3/s	L_{PIG}	2.00	m
ρ_0	5.44	kg/m^3	x_{PIG0}	7,400	m
p_l	7.65	bar	v_{PIG0}	0.00	m/s
Q_l	1.16	m^3/s	F_{fpsta}	2.00	bar
ρ_l	5.20	kg/m^3	F_{fpdyn}	0.33	bar
T	15	℃	F_b	0.00	N

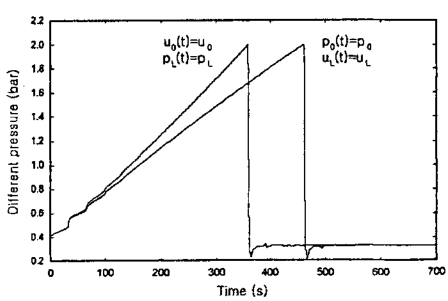

Fig. 6 Different pressure acting on the PIG

4. Simulation Results

Simulation was performed with one pipeline segment in the KOGAS low pressure system, Ueijungboo-Sangye line. The numerical values of system parameters used in this simulation are based on the Korea Gas Corporation (2000) and are given in Table 1. The simulation assumes that the PIG has stopped at a mid-line position by obstruction (debris or deposit), pressure behind the PIG must be increased to overcome both obstructions causing the stoppage and the static friction. Then, the PIG accelerates until the different pressure abates to a level required to overcome the static and dynamic friction.

The sampling time Δt=0.05s and sampling distance Δx=40m are using in this simulation. The following boundary conditions are used: (1) constant flow at inlet $u_0(t)=u_0$ and constant pressure at outlet $p_l(t)=p_l$, (2) constant pressure at inlet $p_0(t)=p_0$ and constant flow at outlet $u_l(t)=u_l$.

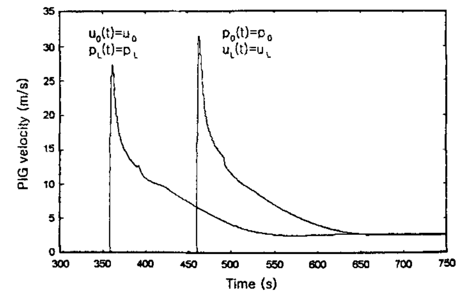

Fig. 7 PIG velocity

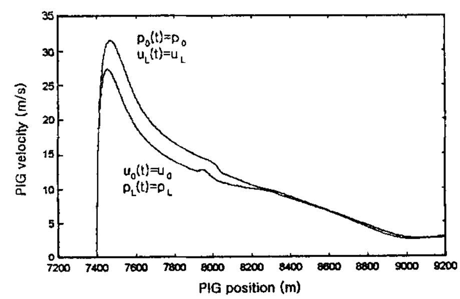

Fig. 8 PIG velocity vs. PIG position

Once the PIG has stopped, pressure increases at its tail and decreases at its nose. These different pressures are plotted in Fig. 6.

Figures 7 and 8 show the PIG velocities vs. time and its positions. The PIG with the boundary conditions of $u_0(t)$ and $p_l(t)$ needs less time for restarting and smaller maximum velocity.

In order to verify the solution accuracy, the calculation was done with reduced sampling time and distance. At each given sampling, the estimate of relative error of maximum velocity of the PIG is calculated as follows(Zwillinger, 1996)

$$error=\frac{|v_{max}^{dt_i}-v_{max}^{dt_{i-1}}|}{v_{max}^{dt_i}}\times 100\%$$

where, $v_{max}^{dt_i}$ and $v_{max}^{dt_{i-1}}$ are the maximum velocities of the PIG calculated with the sampling time dt_i and dt_{i-1} respectively. These errors are plotted in Fig. 9. As shown in this figure, the solution is converged if we choose sampling time enough small. In this simulation, we can choose the sampling time $\Delta t \leq 0.05$s.

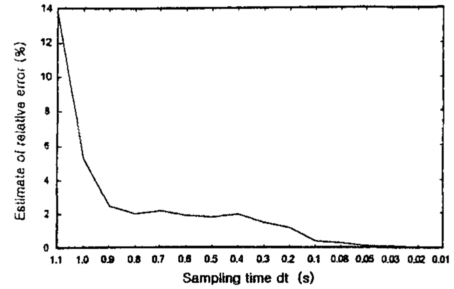

Fig. 9 Estimate of relative error of maximum velocity of the PIG

5. Conclusion

This paper proposes a computational scheme using MOC and regular rectangular grid for estimating the PIG dynamics when it flows in natural gas pipeline. The proposed solution is converged with enough small sampling time and sampling distance. This approach is quite efficient for modelling the rapid flow transient and the PIG dynamics as shown in the simulation results. The PIG dynamics depends on the pipeline operating conditions (ex. boundary conditions). The proposed solution can be used to predict an undesired maximum PIG velocity, and also the PIG dynamics for a given operational condition. Furthermore, it is expected that the modelling results can be used to control the velocity of the PIG in the next study.

Acknowledgement

This paper is a part of a study titled "Modeling and Control of PIG Flow in Natural Gas Pipeline" which is studied by Korea Gas Corporation support. We gratefully acknowledge the contributions and suggestions of related persons.

References

Azevedo L. F. A., Braga A. M. B., Nieckele A. O., Naccache M. F., and Gomes M. G. F. M., 1996, "Simple Hydrodynamic Models for the Prediction of Pig Motions in Pipelines," *Proceedings of the 1996 Offshore Technology Conference*, TX., USA, pp. 729~739.

Cordell J. and Vanzant H., June 1999, "All About Pigging," On-Stream Systems Limited and Hershel Vanzant & Associates.

Fox J. A., 1977, *Hydraulic Analysis of Unsteady Flow in Pipe Networks*, John Wiley & Sons Pub.

Hodge B. K. and Koenig K., 1995, *Compressible Fluid Dynamics with Personal Computer Applications,* Prentice-Hall, Inc., pp. 435~488.

Kentfield J. A. C., 1993, "Nonsteady, One-Dimensional, Internal, Compressible Flows: Theory and Applications," Oxford University Press, pp. 33~118.

Korea Gas Corporation, March 2000, "The First Stage of Development of Intelligent PIG for Low Pressure Pipeline"

Lima P. C. R., Petrobas Petrobas, and Yeoung H., 1999, "Modeling of Pigging Operations," *Proceedings of SPE Annual Technical Conference and Exhibition*, TX., USA, pp. 563~578.

Nguyen T. T., Yoo H. R., Rho Y. W., and Kim S. B., October 2000, "Modeling and Simulation for PIG Flow Control in Natural Gas Pipeline," *Proceedings of the 15th KACC*, pp. 448~.

Out J. M. M., 1993, "On the Dynamics of Pig-Slug Tranis in Gas Pipeline," *OMAE Pipeline Technology, ASME*, Vol. V, pp. 395~403.

Price G. R., McBrien R. K., Rizopoulous S. N., and Golshan H., May 1999, "Evaluating the Effective Friction Factor and Overall Heat Transfer Coefficient During Unsteady Pipeline Operation," *Journal of Offshore Mechanics and Arctic Engineering, ASME*, Vol. 121, pp. 131~136.

Sim W. G. and Park J. H., 1997, "Transient Analysis for Compressible Fluid Flow in Transmission Line by the Method Of Characteristics," *KSME International Journal*, Vol. 11. No. 2, pp. 173~185.

Tannehill J. C., Anderson D. A., and Pletcher R. H., 1997, *Computational Fluid Mechanics and Heat Transfer*, Taylor & Francis Pub.

White F. M., 1999, *Fluid Mechanics*, McGraw-Hill Pub.

Wylie E. B., Streeter V. L. and Suo L., 1993,

Fluid Transients in Systems, Prentice-Hall, Inc.
Zwillinger D., 1996, "Standard Mathematical Tables and Formulae," CRC Press, pp. 716~717.

Appendix

A.1 Calculation of friction force F_f(white, 1999)

Darcy-Weisbach equation is used for finding pipe head loss:

$$h_f = f\frac{L}{d}\frac{u^2}{2g} \tag{a}$$

Darcy (Fanning) friction coefficient f depends on the Reynolds number $Re = u.d/\nu$

i. $Re < 0.1$

$$f = 160$$

ii. $0.1 \le Re \le 2300$

$$f = \frac{64}{Re}$$

iii. $Re > 2300$, the flow is turbulent and f is given by Colebrook-White formula:

$$\frac{1}{\sqrt{f}} = -2\log\left(\frac{2.51}{Re\sqrt{f}} + \frac{k/d}{3.7}\right) \tag{b}$$

and its reasonably good approximation is given by the Haadland formula:

$$\frac{1}{\sqrt{f}} = -1.8\log\left[\frac{6.9}{Re} + \left(\frac{k/d}{3.7}\right)^{1.11}\right] \tag{c}$$

The process of calculating f is suggested as follows:

* Step 1: Calculating f_1 from (c)

$$f_1 = \left\{-1.8\log\left[\frac{6.9}{Re} + \left(\frac{k/d}{3.7}\right)^{1.11}\right]\right\}^{-2}$$

* Step 2: Calculating f from (b)

$$f = \left[-2\log\left(\frac{2.51}{Re\sqrt{f_1}} + \frac{k/d}{3.7}\right)\right]^{-2}$$

* Step 3: If $\|f - f_1\| \le$ [[error] then stop.
  If $\|f - f_1\| >$ [error] then $f_1 = f$ is assigned and go to step 1.

where, [error] is tolerance and can be chosen as 0.01%.

The pressure loss due to friction and the friction force per unit pipe length are given respectively as follows:

$$\Delta p = h_f \rho g = f\frac{L}{d}\frac{u^2}{2}\rho \tag{d}$$

$$F_f = \frac{\Delta p A}{L} = \frac{1}{8}\pi d f \rho u^2 \tag{e}$$